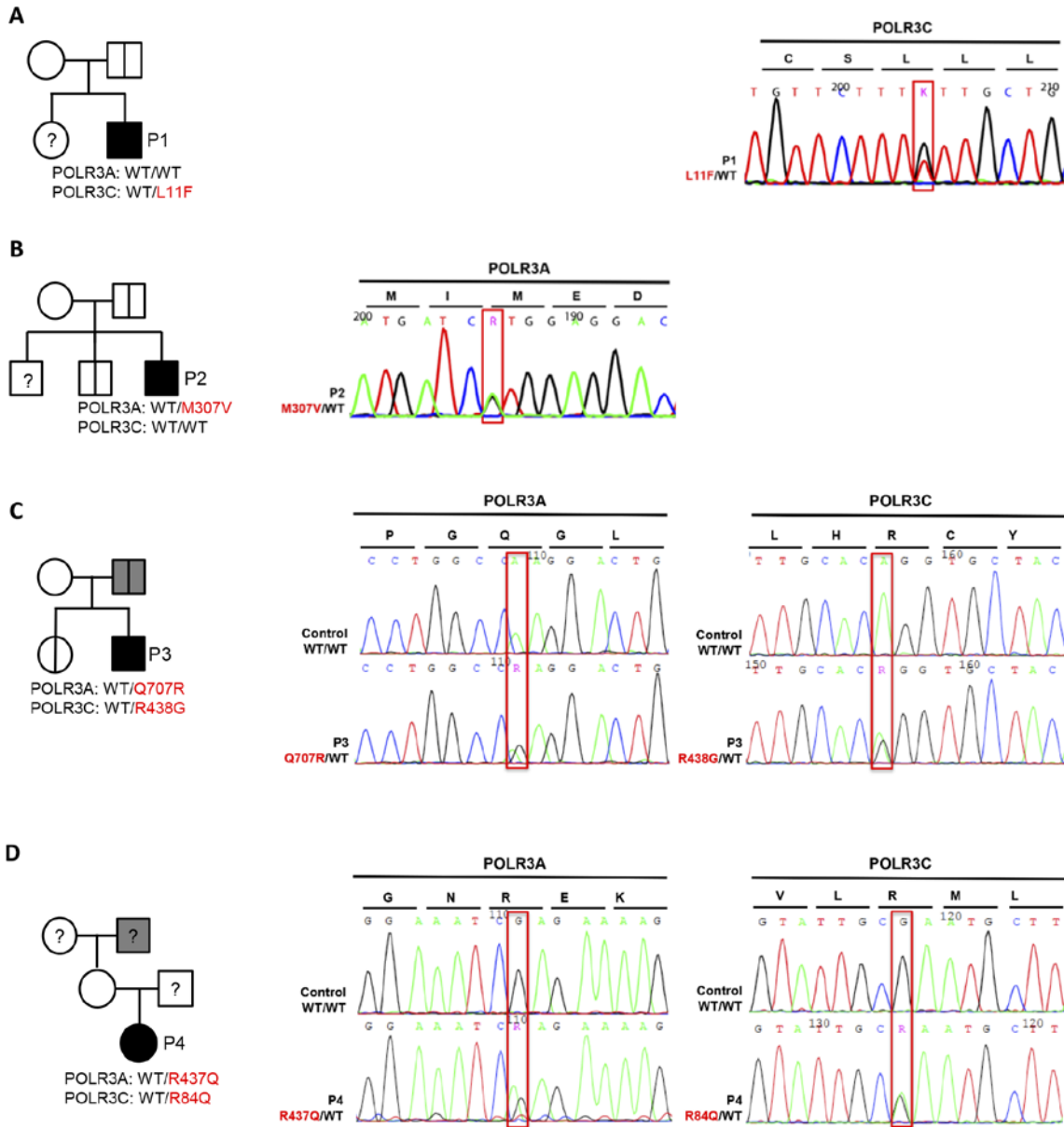


# Supplemental material



**Supplemental Figure 1. Sanger sequencing of *POLR3A* and *POLR3C*.** DNA sequences of the regions in the *POLR3A* and *C* genes carrying the mutations.

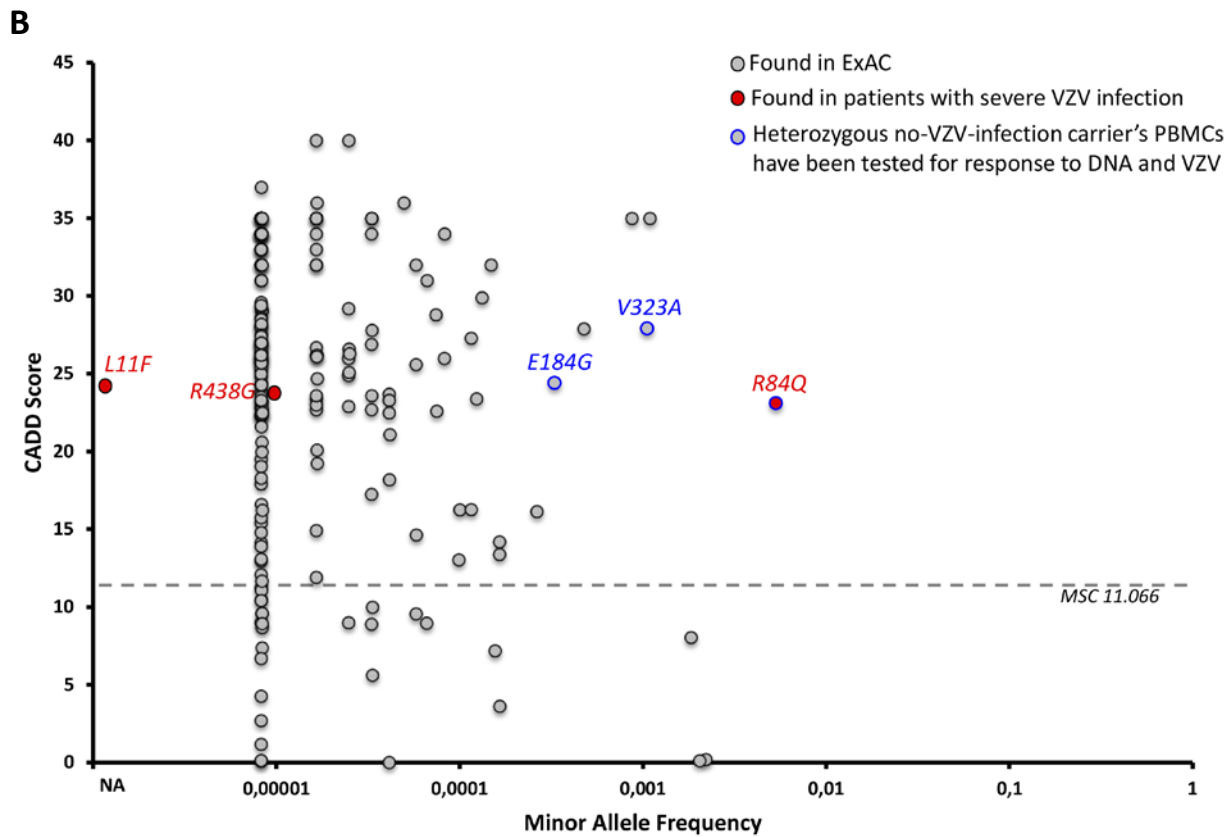
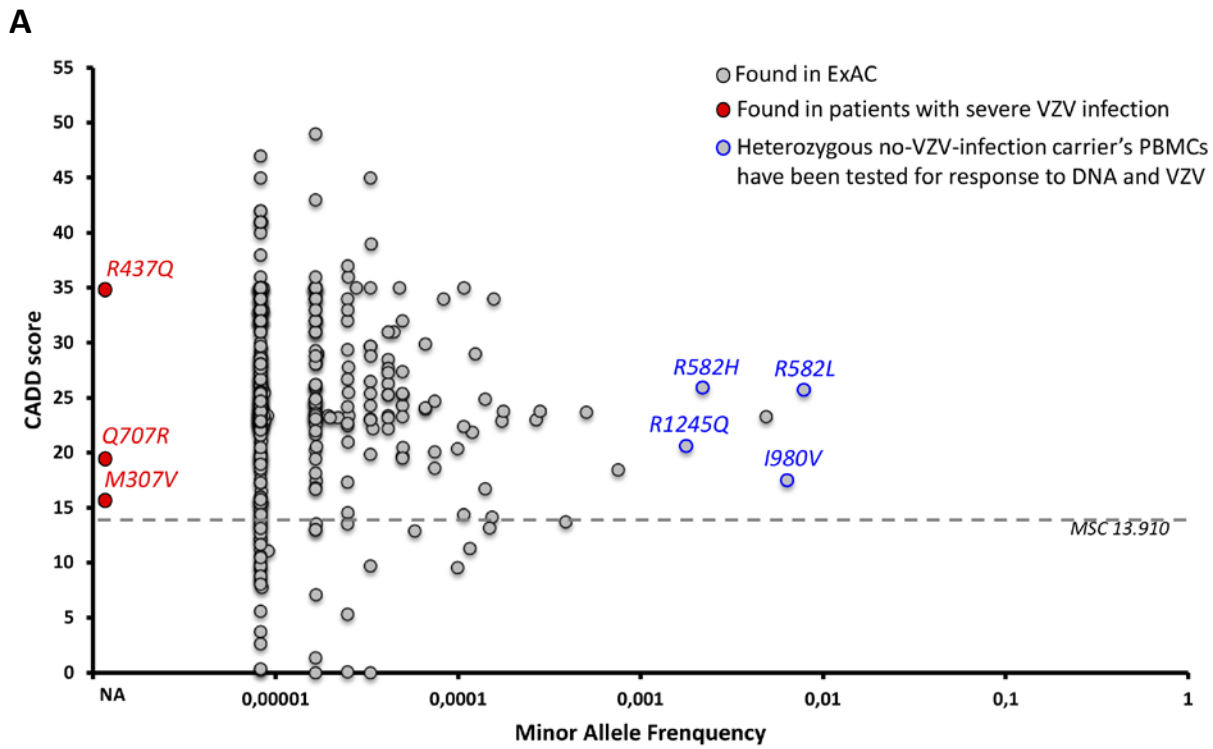
POLR3A

	293	322
<b>P2</b>	IKKHRISGAKTQMIEDWDFLQQLCALYIN	
Homo sapiens	IKKHRISGAKTQMIEDWDFLQQLCALYIN	
Macaca mulatta	IKKHRISGAKTQMIEDWDFLQQLCALYIN	
Pan troglodytes	IKKHRISGAKTQMIEDWDFLQQLCALYIN	
Bos taurus	IKKHRISGAKTQMIEDWDFLQQLCALYIN	
Sus scrofa	IKKHRISGAKTQMIEDWDFLQQLCALYIN	
Equus caballus	IKKHRISGAKTQMIEDWDFLQQLCALYIN	
Oryctolagus cuniculus	IKKHRISGAKTQMIEDWDFLQQLCALYIN	
Rattus norvegicus	IKKHRISGAKTQMIEDWDFLQQLCALYIN	
Mus musculus	IKKHRISGAKTQMIEDWDFLQQLCALYIN	
Otolemur garnettii	IKKHRISGAKTQMIEDWDFLQQLCALYIN	
Monodelphis domestica	IKKHRISGAKTQMIEDWDFLQQLCALYIN	
Papio anubis	IKKHRISGAKTQMIEDWDFLQQLCALYIN	
Callithrix jacchus	IKKHRISGAKTQMIEDWDFLQQLCALYIN	
Canis familiaris	IKKHRISGAKTQMIEDWDFLQQLCALYIN	
Loxodonta africana	IKKHRISGAKTQMIEDWDFLQQLCALYIN	
Ovis aries	IKKHRISGAKTQMIEDWDFLQQLCALYIN	
Felis catus	IKKHRISGAKTQMIEDWDFLQQLCALYIN	
	693	722
<b>P3</b>	NRGFSIGIGDVTPEGLLKAKYELLNAGKY	
Homo sapiens	NRGFSIGIGDVTPEGLLKAKYELLNAGKY	
Macaca mulatta	NRGFSIGIGDVTPEGLLKAKYELLNAGKY	
Pan troglodytes	NRGFSIGIGDVTPEGLLKAKYELLNAGKY	
Bos taurus	NRGFSIGIGDVTPEGLLKAKYELLNAGKY	
Sus scrofa	NRGFSIGIGDVTPEGLLKAKYELLNAGKY	
Equus caballus	NRGFSIGIGDVTPEGLLKAKYELLNAGKY	
Oryctolagus cuniculus	NRGFSIGIGDVTPEGLLKAKYELLNAGKY	
Rattus norvegicus	NRGFSIGIGDVTPEGLLKAKYELLNAGKY	
Mus musculus	NRGFSIGIGDVTPEGLLKAKYELLNAGKY	
Otolemur garnettii	NRGFSIGIGDVTPEGLLKAKYELLNAGKY	
Monodelphis domestica	NRGFSIGIGDVTPEGLLKAKYELLNAGKY	
Papio anubis	NRGFSIGIGDVTPEGLLKAKYELLNAGKY	
Callithrix jacchus	NRGFSIGIGDVTPEGLLKAKYELLNAGKY	
Canis familiaris	NRGFSIGIGDVTPEGLLKAKYELLNAGKY	
Loxodonta africana	NRGFSIGIGDVTPEGLLKAKYELLNAGKY	
Ovis aries	NRGFSIGIGDVTPEGLLKAKYELLNAGKY	
Felis catus	NRGFSIGIGDVTPEGLLKAKYELLNAGKY	
	423	452
<b>P4</b>	QRHTQMK--RFLKYGNREKMAQELKYGDI	
Homo sapiens	QRHTQMK--RFLKYGNREKMAQELKYGDI	
Macaca mulatta	QRHTQMK--RFLKYGNREKMAQELKYGDI	
Pan troglodytes	QRHTQMK--RFLKYGNREKMAQELKYGDI	
Bos taurus	QRHTQMK--RFLKYGNREKMAQELKYGDI	
Sus scrofa	QRHTQMK--RFLKYGNREKMAQELKYGDI	
Equus caballus	QRHTQMK--RFLKYGNREKMAQELKYGDI	
Oryctolagus cuniculus	QRHTQMK--RFLKYGNREKMAQELKYGDI	
Rattus norvegicus	QRHTQMK--RFLKYGNREKMAQELKYGDI	
Mus musculus	QRHTQMK--RFLKYGNREKMAQELKYGDI	
Otolemur garnettii	QRHTQMK--RFLKYGNREKMAQELKYGDI	
Monodelphis domestica	QRHTQMK--RFLKYGNREKMAQELKYGDI	
Papio anubis	QRHTQMK--RFLKYGNREKMAQELKYGDI	
Callithrix jacchus	QRHTQMK--RFLKYGNREKMAQELKYGDI	
Canis familiaris	QRHTQMK--RFLKYGNREKMAQELKYGDI	
Loxodonta africana	QRHTQMK--RFLKYGNREKMAQELKYGDI	
Ovis aries	QRHTQMK--RFLKYGNREKMAQELKYGDI	
Felis catus	QRHTQMK--RFLKYGNREKMAQELKYGDI	

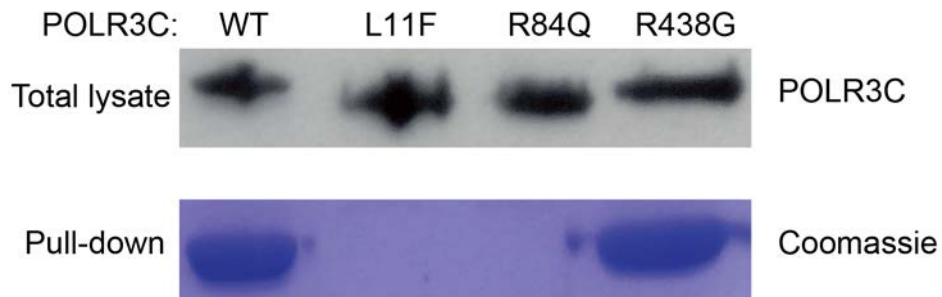
POLR3C

	1	30
<b>P1</b>	MTQAEIKLCSLLQEHFGEIIVEKIGVHLIR	
Homo sapiens	MTQAEIKLCSLLQEHFGEIIVEKIGVHLIR	
Macaca mulatta	MTQAEIKLCSLLQEHFGEIIVEKIGVHLIR	
Pan troglodytes	MTQAEIKLCSLLQEHFGEIIVEKIGVHLIR	
Bos taurus	MTQAEIKLCSLLQEHFGEIIVEKIGVHLIR	
Sus scrofa	MTQAEIKLCSLLQEHFGEIIVEKIGVHLIR	
Equus caballus	MTQAEIKLCSLLQEHFGEIIVEKIGVHLIR	
Oryctolagus cuniculus	MTQAEIKLCSLLQEHFGEIIVEKIGVHLIR	
Rattus norvegicus	MTQAEIKLCSLLQEHFGEIIVEKIGVHLIR	
Mus musculus	MTQAEIKLCSLLQEHFGEIIVEKIGVHLIR	
Otolemur garnettii	MTQAEIKLCSLLQEHFGEIIVEKIGVHLIR	
Monodelphis domestica	MTQAEIKLCSLLQEHFGEIIVEKIGVHLIR	
Papio anubis	MTQAEIKLCSLLQEHFGEIIVEKIGVHLIR	
Callithrix jacchus	MTQAEIKLCSLLQEHFGEIIVEKIGVHLIR	
Canis familiaris	MTQAEIKLCSLLQEHFGEIIVEKIGVHLIR	
Loxodonta africana	MTQAEIKLCSLLQEHFGEIIVEKIGVHLIR	
Ovis aries	MTQAEIKLCSLLQEHFGEIIVEKIGVHLIR	
Felis catus	MTQAEIKLCSLLQEHFGEIIVEKIGVHLIR	
	70	99
<b>P3</b>	RGVVEYEAQCSRVLMRLRYPRYIYTKTLY	
Homo sapiens	RGVVEYEAQCSRVLMRLRYPRYIYTKTLY	
Macaca mulatta	RGVVEYEAQCSRVLMRLRYPRYIYTKTLY	
Pan troglodytes	RGVVEYEAQCSRVLMRLRYPRYIYTKTLY	
Bos taurus	RGVVEYEAQCSRVLMRLRYPRYIYTKTLY	
Sus scrofa	RGVVEYEAQCSRVLMRLRYPRYIYTKTLY	
Equus caballus	RGVVEYEAQCSRVLMRLRYPRYIYTKTLY	
Oryctolagus cuniculus	RGVVEYEAQCSRVLMRLRYPRYIYTKTLY	
Rattus norvegicus	RGVVEYEAQCSRVLMRLRYPRYIYTKTLY	
Mus musculus	RGVVEYEAQCSRVLMRLRYPRYIYTKTLY	
Otolemur garnettii	RGVVEYEAQCSRVLMRLRYPRYIYTKTLY	
Monodelphis domestica	RGVVEYEAQCSRVLMRLRYPRYIYTKTLY	
Papio anubis	RGVVEYEAQCSRVLMRLRYPRYIYTKTLY	
Callithrix jacchus	RGVVEYEAQCSRVLMRLRYPRYIYTKTLY	
Canis familiaris	RGVVEYEAQCSRVLMRLRYPRYIYTKTLY	
Loxodonta africana	RGVVEYEAQCSRVLMRLRYPRYIYTKTLY	
Ovis aries	RGVVEYEAQCSRVLMRLRYPRYIYTKTLY	
Felis catus	RGVVEYEAQCSRVLMRLRYPRYIYTKTLY	
	424	453
<b>P4</b>	YTVNLSAARMLLHCYKSIANLIERRQFE	
Homo sapiens	YTVNLSAARMLLHCYKSIANLIERRQFE	
Macaca mulatta	YTVNLSAARMLLHCYKSIANLIERRQFE	
Pan troglodytes	YTVNLSAARMLLHCYKSIANLIERRQFE	
Bos taurus	YTVNLSAARMLLHCYKSIANLIERRQFE	
Sus scrofa	YTVNLSAARMLLHCYKSIANLIERRQFE	
Equus caballus	YTVNLSAARMLLHCYKSIANLIERRQFE	
Oryctolagus cuniculus	YTVNLSAARMLLHCYKSIANLIERRQFE	
Rattus norvegicus	YTVNLSAARMLLHCYKSIANLIERRQFE	
Mus musculus	YTVNLSAARMLLHCYKSIANLIERRQFE	
Otolemur garnettii	YTVNLSAARMLLHCYKSIANLIERRQFE	
Monodelphis domestica	YTVNLSAARMLLHCYKSIANLIERRQFE	
Papio anubis	YTVNLSAARMLLHCYKSIANLIERRQFE	
Callithrix jacchus	YTVNLSAARMLLHCYKSIANLIERRQFE	
Canis familiaris	YTVNLSAARMLLHCYKSIANLIERRQFE	
Loxodonta africana	YTVNLSAARMLLHCYKSIANLIERRQFE	
Ovis aries	YTVNLSAARMLLHCYKSIANLIERRQFE	
Felis catus	YTVNLSAARMLLHCYKSIANLIERRQFE	

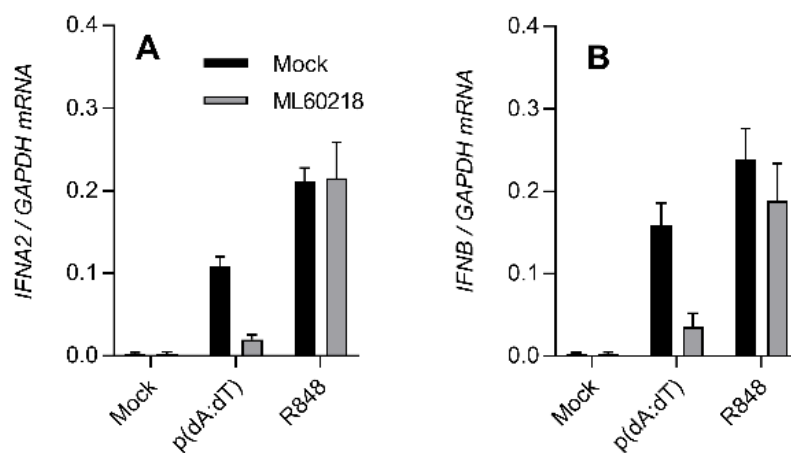
**Supplemental Figure 2. Alignments.** Alignment across species of the regions surrounding the mutations. Residues marked in red, represent the residue in patients. Residues marked in green represent the residue in the human wildtype allele. Residues marked in yellow are not conserved, but have similar physical properties as the conserved residue at the given position.



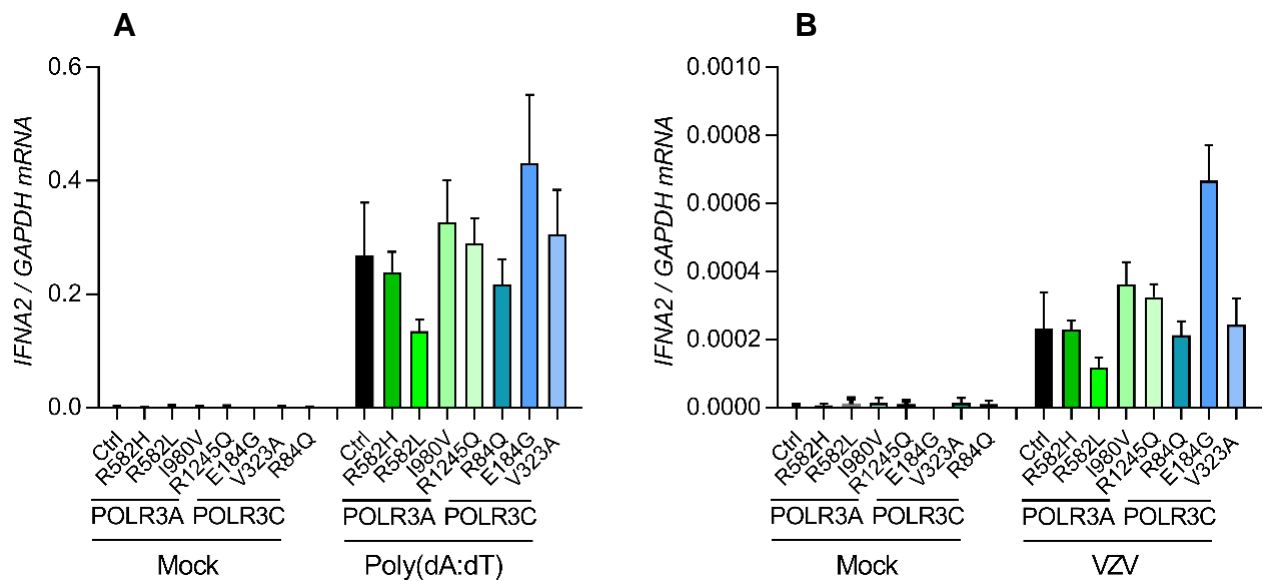
**Supplemental Figure 3. Analysis of CADD score versus allele frequency variations in ExAC and VZV patients. (A) *POLR3A*, (B) *POLR3C*. MSC, Mutation Significance Cutoffs.**



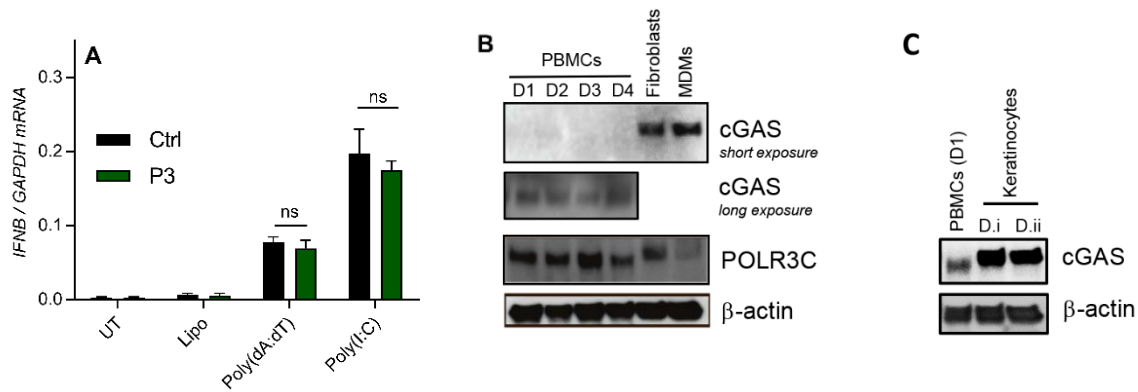
**Supplemental Figure 4. Expression of WT and patient POLR3C in bacteria.** Bacteria were transduced with plasmids encoding WT POLR3C and the 3 mutant forms from P1, P3, and P4 with a His-tag at the N-terminus. POLR3C expression was induced by addition of 1 mM IPTG treatment. Total lysates were analyzed for expression of POLR3C by Western blot, thus demonstrating that all mutants were expressed (top panel). Lysates were collected and evaluated for protein retention by the His-tag Nickel affinity resin.



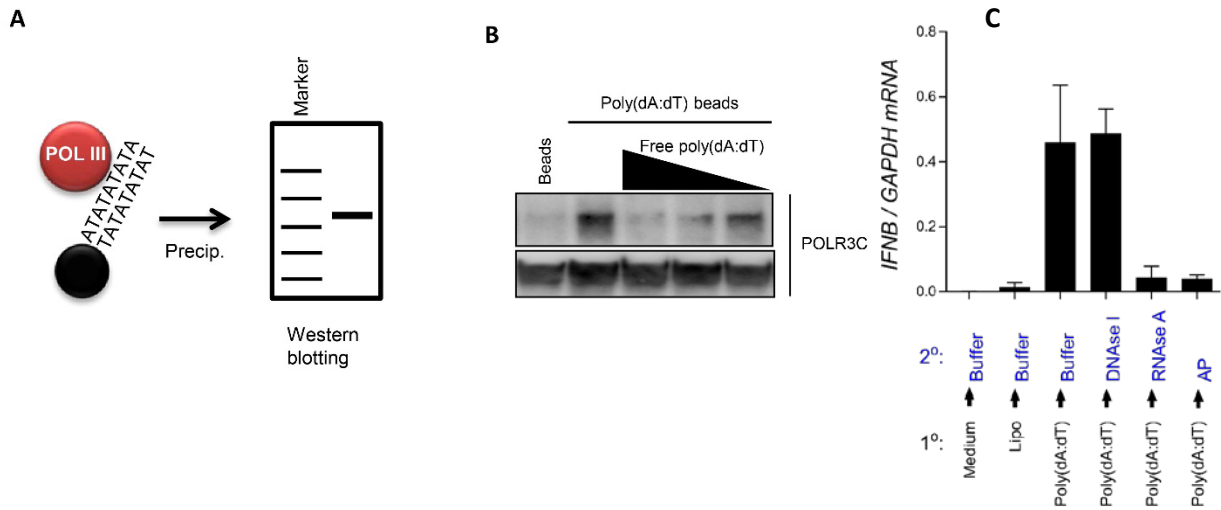
**Supplemental Figure 5. POL III-dependent stimulation of IFN expression by poly(dA:dT) in PBMCs.** PBMCs from a healthy donor were treated with the Pol III inhibitor ML-60218 (10  $\mu$ M) for 16 h prior to transfection of poly(dA:dT) (2  $\mu$ g/mL) or treatment with R848 (1  $\mu$ g/mL). Total RNA was harvested 6 h after stimulation and levels of (A) *IFNA2* and (B) *IFNB* mRNA were determined by RT-qPCR as shown. Data are shown as means  $\pm$  st.dev.



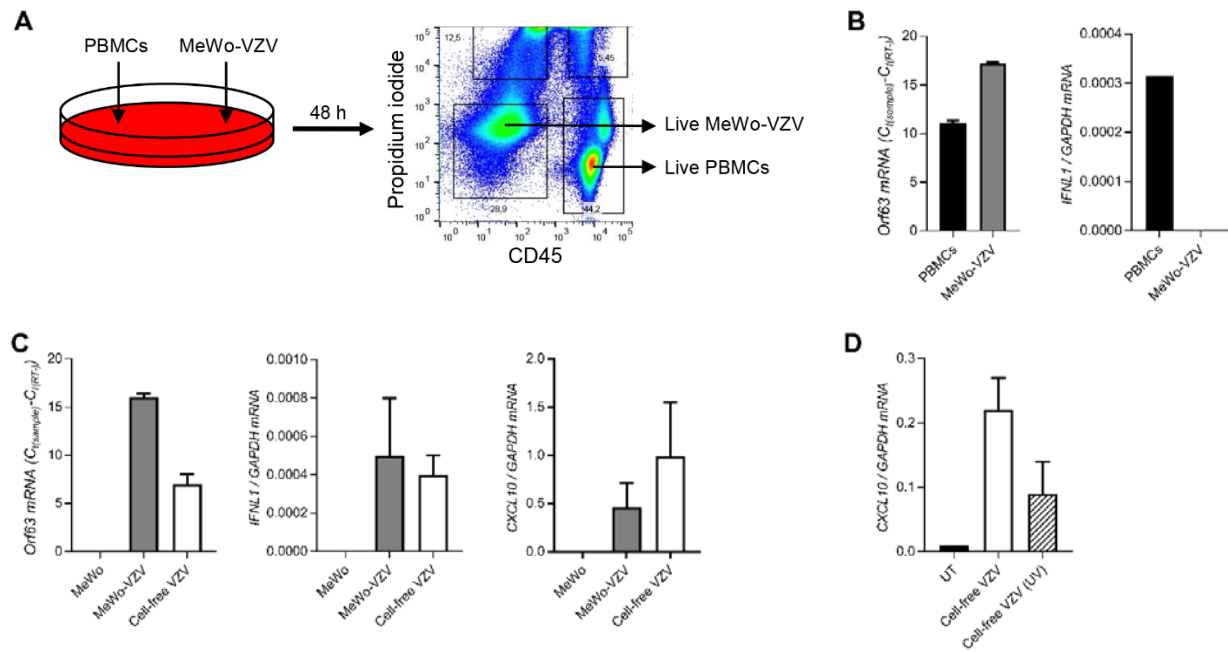
**Supplemental Figure 6. Expression of *IFNA2* by PBMCs from donors with other POLR3 mutations.** PBMCs from donors with other POLR3 mutations than the ones found in the patients were (A) transfected with poly(dA:dT) (2  $\mu$ g/mL), or (B) VZV-infected MeWo cells. Total RNA was harvested 6h after poly(dA:dT) stimulation and 48 h after initiation of co-culture with VZV-MeWo cells. Levels of *IFNA2* mRNA were determined by RT-qPCR as indicated. The levels of cytokine mRNAs were normalized to *GAPDH*, and data are presented as means  $\pm$  st.dev. Ctrl, Control. Average of 4 sex- and age-matched controls.



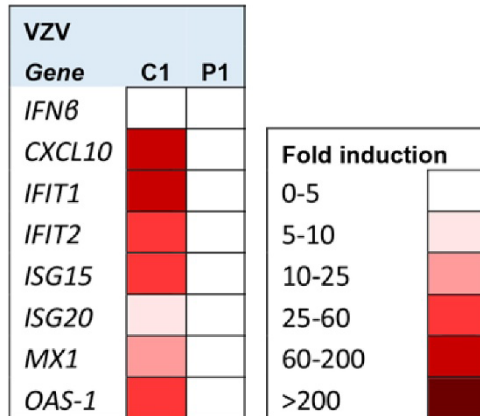
**Supplemental Figure 7. Normal response to DNA in fibroblasts from P3.** Fibroblasts from P3 and a healthy donor were transfected with (A) poly(dA:dT) or poly(I:C) (both 2  $\mu$ g/mL). Total RNA was harvested 6 h later and levels of *IFN $\beta$*  mRNA were determined by RT-qPCR, normalized to *GAPDH*, and presented as means  $\pm$  st.dev. ns,  $p > 0.05$ . (B) Total cell lysates from PBMCs (4 donors), skin fibroblasts, and monocyte-derived macrophages were immunoblotted for the levels of cGAS, POLR3C, and  $\beta$ -actin. (C) Total cell lysates from PBMCs (1 donor), and keratinocytes (2 donors) were immunoblotted for the levels of cGAS and  $\beta$ -actin.



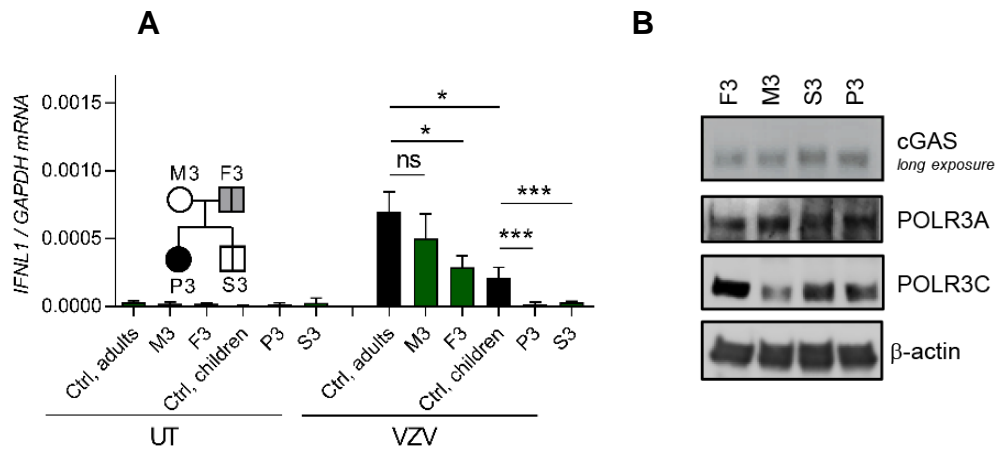
**Supplemental Figure 8. Poly(dA:dT) interacts with POL III and leads to generation of immunostimulatory 5'-triphosphorylated RNA.** (A) Illustration of the principle steps in precipitation and identification of poly(dA:dT)-interacting proteins. (B) Poly(dA:dT) beads incubated with cytoplasmic extracts of PBMCs from a healthy donor in the presence and absence of increasing levels of free poly(dA:dT) were precipitated and immunoblotted with anti-POLR3C. (C) PBMCs from one healthy donor were treated as indicated under 1°. Total RNA was isolated 14 h later, and the RNA was treated as specified under 2° before transfection into HEK293 cells. Total RNA was harvested 6 h later and levels of *IFNB* mRNA were determined by RT-qPCR and normalized to *GAPDH*. Data are presented as means +/- st.dev.



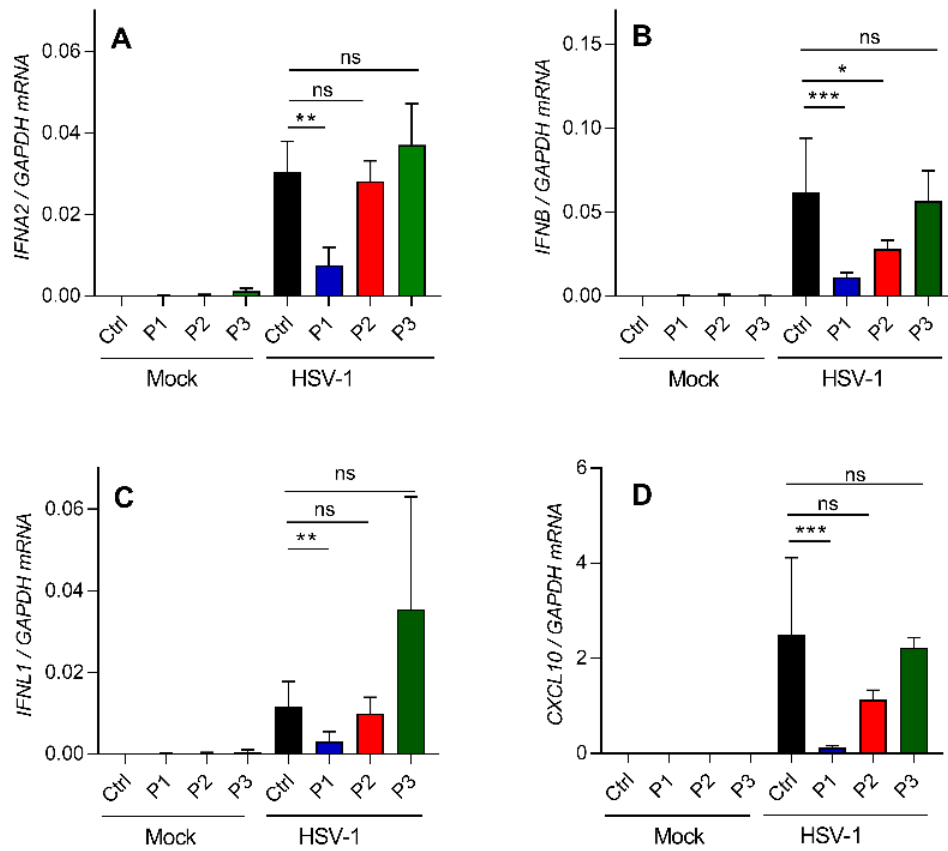
**Supplemental Figure 9. Characterization of the PBMC-MeWo coculture system.** (A, B) PBMCs from a healthy donor were co-cultured with MeWo cells (VZV-infected or non-infected) in a 1:1 ratio. The cells two cell populations were separated 48 h later by sorting for CD45 expression, and levels of *Orf63* and *IFNL1* mRNA were determined by RT-qPCR. (C) PBMCs were co-cultured with (i) uninfected MeWo cells, (ii) VZV-infected MeWo cells in a 1:1 ratio, or (iii) sonicated and cleared lysates from infected MeWo cells (cell-free VZV). (D) In a different experimental set-up PBMCs were co-cultured with cell-free VZV +/- UV-treatment prior to addition to the PBMCs. Total RNA was harvested 12 h after initiation of co-culture/infection, and levels of *Orf63*, *IFNL1*, and *CXCL10* mRNA was determined by RT-qPCR. Data are presented as means +/- st.dev.



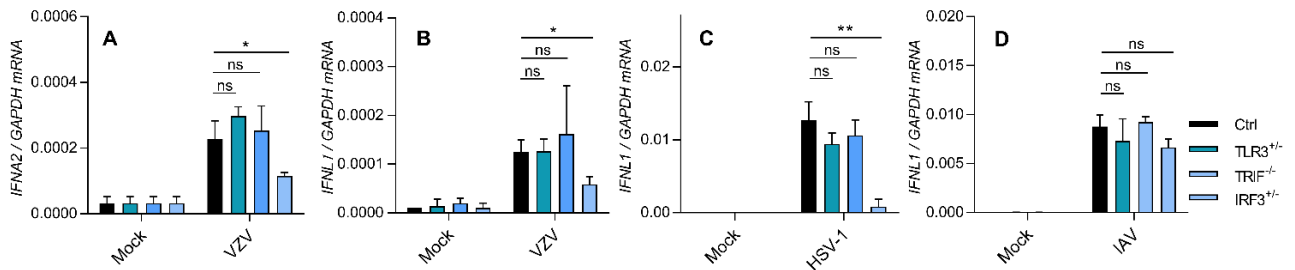
**Supplemental Figure 10. Reduced ISG expression in P1 PBMCs after VZV infection.** PBMCs from P1 and an age- and gender-matched healthy control were treated with VZV-infected MeWo cells for 48 h. Total RNA was harvested and levels of IFN $\beta$  and selected ISGs were determined by Fluidigm. The data were normalized to  $\beta$ -actin levels (which were comparable between the two groups) and are shown as heat-maps, with each color point representing means of 3 biological replicates.



**Supplemental Figure 11. Characterization of *IFNλ1* production in response to VZV infection by PBMCs from the family of P3.** (A) PBMCs from P3, family members, and age-matched healthy controls were treated with VZV-infected MeWo cells. Total RNA was harvested 48 h after initiation of co-culture with VZV-MeWo cells and levels of *IFNλ1* mRNA were determined by RT-qPCR. The levels of the mRNA of interest was normalized to *GAPDH*, and data are presented as means +/- st.dev. Ctrl, Control. Average of 7 and 12 age-matched adult controls in the adult and children groups, respectively. ns,  $p > 0.05$ ; \*,  $0.01 < p < 0.05$ ; \*\*,  $0.01 < p < 0.001$ ; \*\*\*,  $0.001 < p < 0.0001$ . (B) Expression levels of cGAS, POLR3A, POLR3C, and β-actin in PBMCs lysates from the family of P3.



**Supplemental Figure 12. Expression of IFNs and ISGs by PBMCs from P1-P3 after HSV-1 infection.** PBMCs from P1, P2, P3 and healthy controls were infected with HSV-1 (MOI 3). Total RNA was harvested 6 h after infection and levels of (A) *IFNA2*, (B) *IFNB*, (C) *IFNL1*, and (D) *CXCL10* mRNA were determined by RT-qPCR as indicated. The levels of cytokine mRNAs were normalized to *GAPDH*, and data are presented as means +/- st.dev. Ctrl, Control. Average of 4 sex- and age-matched controls. ns,  $p > 0.05$ ; \*,  $0.01 < p < 0.05$ ; \*\*,  $0.01 < p < 0.001$ ; \*\*\*,  $0.001 < p < 0.0001$ .



**Supplemental Figure 13. PBMCs from patients with mutations in TLR3 pathway genes have normal response to VZV infection.** PBMCs from healthy controls and patients with the indicated mutations in genes of the TLR3 pathway were (A, B) treated with VZV-infected MeWo cells, (C) infected with HSV-1 (MOI 3), or (D) IAV (MOI 8). Total RNA was harvested 48 h after initiation of co-culture with VZV-MeWo cells and 6 h after HSV and IAV infections. Levels of *IFNA2* and *IFNL1* mRNA were determined by RT-qPCR as indicated. The levels of the mRNA of interest were normalized to *GAPDH*, and data are presented as means +/- st.dev. Ctrl, Control. Average of 4 age-matched controls. ns,  $p > 0.05$ ; \*,  $0.01 < p < 0.05$ ; \*\*,  $0.01 < p < 0.001$ ; \*\*\*,  $0.001 < p < 0.0001$ .

**Supplemental Table 1. Genes involved in IFN production and function**

<b>Gene symbol</b>	<b>Gene name</b>	<b>HGNC ID</b>	<b>Chromosome Location</b>
<i>ADAR1</i>	Adenosine deaminase	103	1q21.3
<i>AIM2</i>	Absent in melanoma 2	357	1q22
<i>AMFR</i>	Autocrine Motility Factor Receptor	463	16q21
<i>APOBEC3G</i>	apolipoprotein B mRNA editing enzyme catalytic subunit 3G	17357	22q13.1-q13.2
<i>ATF2</i>	Activating transcription factor 2	784	2q32
<i>ATM</i>	Ataxia telangiectasia mutated	795	11q22-q23
<i>BST2</i>	Bone marrow stromal cell antigen 2	1119	19p13.1
<i>BTK</i>	Bruton agammaglobulinemia tyrosine kinase	1133	Xq21.33-q22
<i>CASP1</i>	Caspase 1	1499	11q23
<i>CASP10</i>	Caspase 10	1500	2q33-q34
<i>CASP8</i>	Caspase 8	1509	2q33-q34
<i>CD74</i>	CD74	1697	5q32
<i>CHUK</i>	Conserved helix-loop-helix ubiquitous kinase / Nuclear Factor NF-Kappa-B Inhibitor Kinase Alpha	1974	10q24-q25
<i>CIITA</i>	Class II, major histocompatibility complex, transactivator	7067	16p13
<i>CXCL9</i>	C-X-C motif chemokine ligand 9	4283	4q21
<i>CXCL10</i>	C-X-C motif chemokine ligand 10	3627	4q21
<i>CXCL11</i>	C-X-C motif chemokine ligand 11	6373	4q21.2
<i>DDX41</i>	DEAD (Asp-Glu-Ala-Asp) box polypeptide 41	18674	5q35.3
<i>DDX58</i>	DEAD (Asp-Glu-Ala-Asp) box polypeptide 58 (RIG-I)	23586	9p12
<i>DDX60</i>	DEAD (Asp-Glu-Ala-Asp) box polypeptide 58	25942	4q32.3
<i>DHX9</i>	DEAH-box helicase 9	2750	1q25
<i>DHX36</i>	DEAH-box helicase 36	14410	3q25.2
<i>DHX58</i>	DEAH-box helicase 58 (LGP2)	29517	17q21.2
<i>DOCK2</i>	Dedicator of cytokinesis 2	1794	5q35.1
<i>DOCK8</i>	Dedicator of cytokinesis 8	19191	9p24.3
<i>GBP1</i>	Guanylate binding protein 1	4182	1p22.2
<i>GBP2</i>	Guanylate binding protein 2	4183	1p22.2
<i>GATA2</i>	GATA binding protein 2	4171	3q21
<i>HPSE</i>	Heparanase	5164	4q21.3
<i>IFI6</i>	Interferon alpha inducible protein 6	4054	1p35
<i>IFI16</i>	Interferon, gamma-inducible protein 16	5395	1q22
<i>IFIH1</i>	Interferon induced with helicase C domain 1 (MDA5)	18873	2q24.2
<i>IFIT1</i>	Interferon induced protein with tetratricopeptide repeats 1	5407	10q23.31
<i>IFIT2</i>	Interferon induced protein with tetratricopeptide repeats 2	5409	10q23.31
<i>IFIT3</i>	Interferon induced protein with tetratricopeptide repeats 3	5411	10q24

<i>IFITM1</i>	Interferon induced transmembrane protein 1	5412	11p15.5
<i>IFITM2</i>	Interferon induced transmembrane protein 2	5413	11p15.5
<i>IFITM3</i>	Interferon induced transmembrane protein 3	5414	11p15.5
<i>IFNA1</i>	Interferon alpha1	3439	9p22
<i>IFNA2</i>	Interferon alpha2	3440	9p22
<i>IFNA4</i>	Interferon alpha4	3441	9p22
<i>IFNA5</i>	Interferon alpha5	3442	9p22
<i>IFNA6</i>	Interferon alpha6	3443	9p22
<i>IFNA7</i>	Interferon alpha7	3444	9p22
<i>IFNA8</i>	Interferon alpha8	3445	9p22
<i>IFNA10</i>	Interferon alpha10	3446	9p22
<i>IFNA13</i>	Interferon alpha13	3447	9p22
<i>IFNA14</i>	Interferon alpha14	3448	9p22
<i>IFNA16</i>	Interferon alpha16	3449	9p22
<i>IFNA17</i>	Interferon alpha17	3451	9p22
<i>IFNA21</i>	Interferon alpha21	3452	9p22
<i>IFNAR1</i>	Interferon alpha and beta receptor subunit 1	3454	21q22.11
<i>IFNAR2</i>	Interferon alpha and beta receptor subunit 1	3455	21q22.11
<i>IFNB1</i>	Interferon, beta1	3456	9p21
<i>IFNG</i>	Interferon gamma	5438	12q14
<i>IFNGR1</i>	Interferon gamma receptor 1	5439	6q23-q24
<i>IFNGR2</i>	Interferon gamma receptor 2 (interferon gamma transducer 1)	5440	21q22.1
<i>IFNL1</i>	Interferon lambda 1	18363	19q13.13
<i>IFNL2</i>	Interferon lambda 2	18364	19q13.13
<i>IFNL3</i>	Interferon lambda 3	18365	19q13.13
<i>IFNL4</i>	Interferon lambda 4	44480	19q13.12
<i>IFNLR1</i>	Interferon lambda receptor 1	18584	1p36.11
<i>IKBKB</i>	Inhibitor of kappa light polypeptide gene enhancer in B-cells, kinase beta	5960	8p11.2
<i>IKBKE</i>	Inhibitor of kappa light polypeptide gene enhancer in B-cells, kinase epsilon	14552	1q31
<i>IKBKG</i>	Inhibitor of kappa light polypeptide gene enhancer in B-cells, kinase gamma	5961	Xq28
<i>IL10RB</i>	interleukin 10 receptor subunit beta	5965	21q22.11
<i>IL1RN</i>	Interleukin 1 receptor antagonist	6000	2q14.2
<i>IRAK1</i>	Interleukin-1 receptor-associated kinase 1	3654	Xq28
<i>IRAK2</i>	Interleukin-1 receptor-associated kinase 2	3656	3p25.3
<i>IRAK4</i>	Interleukin-1 receptor-associated kinase 4	17967	12q12
<i>IRF1</i>	Interferon regulatory factor 1	6116	5q31.1
<i>IRF3</i>	Interferon regulatory factor 3	6118	19q13.3-q13.4
<i>IRF5</i>	Interferon regulatory factor 5	6210	7q32
<i>IRF7</i>	Interferon regulatory factor 7	6122	11p15.5
<i>IRF8</i>	Interferon regulatory factor 8	5358	16q24.1

<i>IRF9</i>	Interferon regulatory factor 9	6131	14q11.2
<i>ISG15</i>	Interferon stimulated gene 15, ubiquitin-like modifier	4053	1p36.33
<i>ISG20</i>	Interferon stimulated gene 20, exonuclease	6130	15q26
<i>JAK1</i>	Janus kinase 1	6190	1p32.3-p31.3
<i>JAK2</i>	Janus kinase 2	3717	9p24
<i>JAK3</i>	Janus kinase 3	6193	19p13-p12
<i>MB21D1</i>	Mab-21 domain containing 1 (cGAS)	21367	6q13
<i>MAP3K14</i>	Mitogen-activated protein kinase kinase 14	6853	17q21
<i>MAVS</i>	Mitochondrial antiviral signaling protein	29233	20p13
<i>MRE11A</i>	MRE11 meiotic recombination 11 homolog A ( <i>S. cerevisiae</i> )	7230	11q21
<i>MYD88</i>	Myeloid differentiation primary response 88	7562	3p22
<i>MX1</i>	MX dynamin like GTPase 1	7532	21q22.3
<i>MX2</i>	MX dynamin like GTPase 2	7533	21q22.3
<i>NAMPT</i>	Nicotinamide phosphoribosyltransferase	30092	7q22.3
<i>NFKB2</i>	Nuclear factor of kappa light polypeptide gene enhancer in B-cells 2 (p49/p100)	7795	10q24
<i>NFKBIA</i>	Nuclear factor of kappa light polypeptide gene enhancer in B-cells inhibitor, alpha	7797	14q13
<i>NHEJ1</i>	Nonhomologous end-joining factor 1	25737	2q35
<i>NLRP12</i>	NLR family, pyrin domain containing 12	22938	19q13.42
<i>NLRP2</i>	NLR family, pyrin domain containing 2	22948	19q13.42
<i>NLRP3</i>	NLR family, pyrin domain containing 3	16400	1q44
<i>NOD2</i>	Nucleotide-binding oligomerization domain containing 2	5331	16q12
<i>OAS1</i>	2'-5'-oligoadenylate synthetase 1	8086	12q24.2
<i>OAS2</i>	2'-5'-oligoadenylate synthetase 2	8087	12q24.2
<i>OAS3</i>	2'-5'-oligoadenylate synthetase 3	8088	12q24.2
<i>OASL</i>	2'-5'-oligoadenylate synthetase like	8090	12q24.2
<i>PGM3</i>	Phosphoglucomutase 3	8907	6q14.1-q15
<i>PACT</i>	Protein activator of PKR	9438	2q31.2
<i>PKR</i>	Protein kinase activated by double-stranded RNA	2p22-p21	2p22-p21
<i>POLR3A</i>	RNA polymerase III subunit A	30074	10q22.3
<i>POLR3B</i>	RNA polymerase III subunit B	30348	12q23.3
<i>POLR3C</i>	RNA polymerase III subunit C	30076	1q21
<i>POLR3D</i>	RNA polymerase III subunit D	1080	8q21
<i>POLR3E</i>	RNA polymerase III subunit E	30347	16p12.2
<i>POLR3F</i>	RNA polymerase III subunit F	15763	20p11.23
<i>POLR3G</i>	RNA polymerase III subunit G	30075	5q14.3
<i>POLR3H</i>	RNA polymerase III subunit H	30349	22q13.2
<i>POLR3GL</i>	RNA polymerase III subunit G like	28466	1q21.1
<i>POLR3K</i>	RNA polymerase III subunit K	14121	16p13.3
<i>PRKDC</i>	Protein kinase, DNA-activated, catalytic polypeptide	9413	8q11
<i>PYCARD</i>	PYD and CARD domain containing	16608	16p11.2
<i>RELA</i>	RELA proto-oncogene, NF-kB subunit	9955	11q13
<i>RHBDF2</i>	Rhomboid 5 homolog 2 (iRhom2)	20788	17q25.1

<i>RIPK1</i>	Receptor (TNFRSF)-interacting serine-threonine kinase 1	10019	6p25.2
<i>RIPK3</i>	Receptor-interacting serine-threonine kinase 3	10021	14q12
<i>RNaseH2A</i>	ribonuclease H2 subunit A	18518	19p13.2
<i>RNaseH2B</i>	ribonuclease H2 subunit B	25671	13q14.3
<i>RNaseH2C</i>	ribonuclease H2 subunit C	24116	11q13.1
<i>RNASEL</i>	Ribonuclease L	6041	1q25
<i>RNF135</i>	Ring Finger protein 135	21158	17q11.2
<i>RTP4</i>	receptor transporter protein 4	23992	3q27.3
<i>SAMHD1</i>	SAM and HD domain containing deoxynucleoside triphosphate triphosphohydrolase 1	15925	20pter-q12
<i>STAT1</i>	Signal transducer and activator of transcription 1, 91kDa	11362	2q32.2-q32.3
<i>STAT2</i>	Signal transducer and activator of transcription 2	11363	12q13.3
<i>STAT3</i>	Signal transducer and activator of transcription 3 (acute-phase response factor)	11364	17q21
<i>STAT4</i>	Signal transducer and activator of transcription 4	11365	2q32.2-q32.3
<i>STAT5A</i>	Signal transducer and activator of transcription 5A	11366	17q11.2
<i>STAT5B</i>	signal transducer and activator of transcription 5B	11367	17q11.2
<i>TANK</i>	TRAF family member-associated NFkB activator	11562	2q24-q31
<i>TBK1</i>	TANK-binding kinase 1	11584	12q14.2
<i>TICAM1</i>	Toll-like receptor adaptor molecule 1 (TRIF)	18348	19p13.3
<i>TICAM2</i>	Toll-like receptor adaptor molecule 2 (TRIF)	21354	5q23.1
<i>TIRAP</i>	Toll-interleukin 1 receptor (TIR) domain containing adaptor protein	17192	11q24.2
<i>TLR2</i>	Toll-like receptor 2	11848	4q32
<i>TLR3</i>	Toll-like receptor 3	11849	4q35
<i>TLR4</i>	Toll-like receptor 4	11850	9q33.1
<i>TLR7</i>	Toll-like receptor 7	15631	Xp22.3
<i>TLR8</i>	Toll-like receptor 8	15632	Xp22
<i>TLR9</i>	Toll-like receptor 9	15633	3p21.3
<i>TMEM173</i>	Transmembrane protein 173 (STING)	27962	5q31.2
<i>TRAF3</i>	TNF receptor-associated factor 3	12033	14q32.32
<i>TRAF6</i>	TNF receptor-associated factor 6, E3 ubiquitin protein ligase	12036	11p12
<i>TRIM5</i>	Tripartite motif containing 5	16276	11p15
<i>TRIM19</i>	Tripartite motif containing 19	9113	15q22
<i>TRIM21</i>	Tripartite motif containing 21	11312	11p15.5
<i>TRIM22</i>	Tripartite motif containing 22	16367	11p15
<i>TRIM25</i>	Tripartite motif containing 25	12932	17q23.2
<i>TRIM32</i>	Tripartite motif containing 32	16380	9q33.1
<i>TRIM56</i>	Tripartite motif containing 56	19028	7q22.1

<i>TREX1</i>	Three prime repair exonuclease 1	12269	3p21.31
<i>TYK2</i>	Tyrosine kinase 2	12440	19p13.2
<i>UNC93B1</i>	Unc-93 homolog B1 (C. elegans)	13481	11q13.2
<i>VPS45</i>	Vacuolar protein sorting 45 homolog (S. cerevisiae)	14579	1q21.2
<i>XIAP</i>	X-linked inhibitor of apoptosis	592	Xq25
<i>XRCC5</i>	X-ray repair cross complementing 5	12833	2q35
<i>XRCC6</i>	X-ray repair cross complementing 6	4055	22q13.2
<i>ZBP1</i>	Z-DNA binding protein 1	16176	20q13.31
<i>ZDHHC1</i>	Zinc Finger DHHC-Type Containing 1	17916	16q22.1

---

**Supplemental Table 2. Enrichment of rare POLR3A, POLR3C variations in severe acute VZV infection cohort**

	VZV cohort (21 individuals)	Control cohort (3724 individuals)	VZV vs Control <i>p-value</i>
<b>POLR3A</b>	3	54	0.0020
<b>POLR3C</b>	2	14	0.0046
<b>POLR3A or POLR3C</b>	4	68	0.00036
<b>POLR3A and POLR3C*</b>	2	4	0.0012

Notes:

1. Ethnic origin of the whole-exome/genome-sequenced individuals, from the VZV cohort or from Control cohort, has been assessed by principal component analysis (PCA) using their exome data. The VZV cohort contains 14 Caucasians, 4 North Africans, 1 African, and 2 Americans. The Control cohort was constructed by including individuals from the Human Genetics of Infectious Diseases (HGID) lab no-viral infection cohorts and from the 1000Genome database <sup>(1)</sup>.
2. The 'Control cohort' consists of 1220 individuals from the no-viral infection cohorts of the HGID lab, and 2504 individuals from the 1000Genome project. Total number of individuals in the cohort of severe acute VZV infection or the Control cohort is indicated under the name of each cohort.
3. Under a POLR3A or POLR3C monogenic model, rare alleles with a MAF<0.0001 in ExAC, and with a CADD score higher than predicted Mutational Significance Cut-off of 95% confidence (13.910 for *POLR3A*, 11.066 for *POLR3C*) were considered in the test. Under a POLR3A and POLR3C digenic model\*, rare alleles with a MAF<0.01 in ExAC, and with a CADD score higher than predicted Mutational Significance Cut-off of 95% confidence were considered in the test.
4. Number of individuals from VZV cohort or Control cohort who harbor rare *POLR3A* or *POLR3C* variations is listed in the table.
5. Ethnic-adjusted *POLR3A* and/or *POLR3C* mutation enrichment assessment was performed using logistic regression adjusting on the three first components of the PCA.

Reference:

Genomes Project, C., Auton, A., Brooks, L.D., Durbin, R.M., Garrison, E.P., Kang, H.M., Korbel, J.O., Marchini, J.L., McCarthy, S., McVean, G.A., et al. 2015. A global reference for human genetic variation. *Nature* 526:68-74.

**Supplemental Table 3. Clinical data**

Patient # (sex, age)	Clinical presentation	Paraclinical findings	MR/EEG findings	Diagnosis and treatment
1 (M, 3 years)	- Fever - Convulsions, day 6 - Loss of consciousness - Hypertonia - Anisocoria - Meningism	- VZV PCR (CSF <sup>1</sup> ), + <sup>2</sup> - WBC <sup>3</sup> , 50 cells/ $\mu$ l - Glucose and protein, N <sup>4</sup>	- Brain CAT <sup>7</sup> , N - MRI (4 mo), N - EEG, slowed	Encephalitis Acyclovir 330 mg x3 i.v. for 21 days Day 14: methylprednisolone pulse therapy for 3 days
2 (M, 5 years )	- Ataxia and nystagmus during chickenpox - Chickenpox twice	- VZV PCR (CSF), $\pm$ <sup>5</sup>	MRI: Arnold-Chiari type I with tonsillar herniation	Cerebellitis
3 (M, 5 years)	- diffuse necrotic varicella - severe pneumonia	VZV PCR (TSM) <sup>6</sup> , +		Pneumonitis ECMO support needed
4 (F, 11 years)	- bitemporofrontal acute headache - varicella at 6 years old	- VZV PCR (CSF), +		Encephalitis

<sup>1</sup> CSF, *Cerebrospinal fluid*

<sup>2</sup> +, *positive*;  $\pm$ , *negative*

<sup>3</sup> WBC, *White blood cells*

<sup>4</sup> N, *Normal*

<sup>5</sup> It has been reported that only a minority of patients with VZV cerebellitis harbor detectable levels of viral DNA in the CSF (1). Therefore, since the onset and resolution of the clinical symptoms of cerebellitis coincided with the chickenpox, it was considered highly likely that VZV was the cause of the CNS symptoms.

<sup>6</sup> Tracheal suction material

<sup>7</sup> CAT, *Computed Axial Tomography*; MRI, *Magnetic resonance imaging*; EEG, *Electroencephalography*

1. Rack, A.L. *et al.* Neurologic varicella complications before routine immunization in Germany. *Pediatr. Neurol.* **42**, 40-48 (2010).

**Supplemental Table 4. Immunophenotyping of available patient blood cells**

	<b>P1</b>	<b>P2</b>	<b>VZV patient (no POL III mutation)</b>	<b>Normal range</b>
<b>Hematology</b>				
Neutrophils	3.96 x 10 <sup>9</sup> cells/L	6.43 x 10 <sup>9</sup> cells/L	2.57 x 10 <sup>9</sup> cells/L	1.8-8.0 x 10 <sup>9</sup> cells/L
Lymphocytes	2.86 x 10 <sup>9</sup> cells/L	2.72 x 10 <sup>9</sup> cells/L	3.05 x 10 <sup>9</sup> cells/L	1.2-6.5 x 10 <sup>9</sup> cells/L
Monocytes	0.96 x 10 <sup>9</sup> cells/L	0.73 x 10 <sup>9</sup> cells/L	0.64 x 10 <sup>9</sup> cells/L	0.1-0.8 x 10 <sup>9</sup> cells/L
Eosinophils	0.13 x 10 <sup>9</sup> cells/L	0.19 x 10 <sup>9</sup> cells/L	0.75 x 10 <sup>9</sup> cells/L	0-0.5 x 10 <sup>9</sup> cells/L
Basophils	0.03 x 10 <sup>9</sup> cells/L	0.03 x 10 <sup>9</sup> cells/L	0.02 x 10 <sup>9</sup> cells/L	0.02-0.1x10 <sup>9</sup> cells/L
<b>Flow cytometry</b>				
<i>T cells</i>				
CD3+	1945 cells /μL	1706 cells /μL	1937 cells /μL	700-4200 cells /μL
CD3+CD4+	826 cells /μL	1100 cells /μL	1075 cells /μL	300-2000 cells /μL
CD3+CD8+	889 cells /μL	491 cells /μL	692 cells /μL	300-1800 cells /μL
CD4+/CD8+	0.93	2.24	1.55	0.9 – 2.6
<i>NK cells</i>				
CD16+CD56+CD3÷	191 cells /μL	593 cells /μL	485 cells /μL	90-900 cells /μL
<i>B cells</i>				
CD19+	167 cells /μL	462 cells /μL	492 cells /μL	200-1600 cells /μL
Kappa	53.7% of CD19+	NA	66.9% of CD19+	
Lambda	46.3% of CD19+	NA	33.2% of CD19+	
Kappa/Lambda	1.16	NA	2.02	0.26 - 1.65
CD10	0.5% of CD19+	NA	0.9% of CD19+	
<i>Plasma cells</i>				
CD38++	0.2%	NA	0.1%	
<i>Granulocytes</i>	55.4%	65.1%	65.1%	35-80%

NA, information no available

**Supplemental Table 5. Structural characteristics of the POL III mutations**

<b>Patient, mutation</b>	<b>Localization</b>	<b>Comments</b>
P1, POLR3C L11F	Relatively buried in the core of the protein	May alter the local or general folding of POLR3C
P2, POLR3A M307V	At the interface between POLR3A and POLR3C	May perturb the interaction with POLR3C and its partners, POLR3F and POLR3G
P3, POLR3A Q707R	Exposed to the solvent	May perturb the interaction with associated factors
P3, POLR3C R438G	At the interface with POLR3F	May alter the POLR3C-POLR3F interaction
P4, POLR3A R437Q	Exposed to the solvent	May perturb the interaction with associated factors
P4, POLR3C R84Q	Buried in the core of the protein	May alter folding of POLR3C

**Supplemental Table 6. Summary of phenotypes in PBMCs**

<b>Patient</b>	<b>Genotype</b>	Poly(dA:dT)				VZV			
		<i>IFNA2</i>	<i>IFNB</i>	<i>IFNL1</i>	<i>CXCL10</i>	<i>IFNA2</i>	<i>IFNL1</i>	<i>CXCL10</i>	<i>Orf63</i>
P1	POLR3C L11F	R <sup>1</sup>	R	R, resc <sup>2</sup>	R	N	R, resc	R <sup>3</sup>	E, resc
P2	POLR3A M307V	R	R	R	R	N	N	N	N
P3	POLR3A Q707R, POLR3C R438Q	R	R	R, resc	R	R	R, resc	R	E, resc
P4	POLR3A R437Q POLR3C R84Q	R	R	R	R	R	R	R	E

<sup>1</sup> R, reduced compared to controls; N, normal; E, elevated compared to controls

<sup>2</sup> resc, rescue of phenotype by transduction with wildtype allele

<sup>3</sup> VZV-infected PBMCs from P3 displayed reduced expression of a panel of IFN-stimulated genes compared to controls